Effects of the Core Lipid on the Energetics of Binding of ApoA-I to Model Lipoprotein Particles of Different Sizes†

Masafumi Tanaka,‡ Hiroyuki Saito,‡,§ Padmaja Dhanasekaran,‡ Suzanne Wehrli,‡ Tetsurou Handa,‖ Sissel Lund-Katz,‡ and Michael C. Phillips*,‡

The Children's Hospital of Philadelphia, University of Pennsylvania School of Medicine, Philadelphia, Pennsylvania 19104-4318, and Graduate School of Pharmaceutical Sciences, Kyoto University, Sakyo-ku, Kyoto 606-8501, Japan

Received May 9, 2005; Revised Manuscript Received June 16, 2005

ABSTRACT: Interaction of apolipoproteins (apo) with lipid surfaces plays crucial roles in lipoprotein metabolism and cholesterol homeostasis. To elucidate the thermodynamics of binding of apoA-I to lipid, we used lipid emulsions composed of triolein (TO) and egg phosphatidylcholine (PC) as lipoprotein models. Determination of the level of binding of wild-type (WT) apoA-I and some deletion mutants to large (120 nm diameter; LEM) and small (35 nm diameter; SEM) emulsions indicated that N-terminal (residues 44−65) and C-terminal (residues 190−243 and 223−243) deletions have large effects on lipid interaction, whereas deletion of the central region (residues 123−166) has little effect. Substitution of amino acids at either L230 or L230, L233, and Y236 with proline residues also decreases the level of binding, indicating that an α-helix conformation in this C-terminal region is required for efficient lipid binding. Calorimetry showed that binding of WT apoA-I to SEM generates endothermic heat ($\Delta H \sim 30$ kcal/mol) in contrast to the exothermic heat (ca. −85 kcal/mol) generated upon binding to LEM and egg PC small unilamellar vesicles (SUV). This exothermic heat arises from an ∼25% increase in α-helix content, and it drives the binding of apoA-I to LEM and SUV. There is a similar increase in α-helix content of apoA-I upon binding to either SEM or SUV, but the binding of apoA-I to SEM is an entropy-driven process. These results suggest that the presence of a core triglyceride modifies the highly curved SEM surface packing and thereby the thermodynamics of apoA-I binding in a manner that compensates for the exothermic heat generated by α-helix formation.

High-density lipoproteins (HDL)[1] and its major protein component, apolipoprotein (apo) A-I, have anti-atherogenic properties because of their roles in the reverse cholesterol transport pathway (*1*, *2*). In this pathway, excess cholesterol in peripheral tissues is removed by HDL and lipid-free or lipid-poor apoA-I and transferred to the liver for excretion in bile (*3*, *4*). ApoA-I is involved in every step of the reverse cholesterol transport pathway. Thus, the release of cellular lipids to apoA-I and formation of nascent HDL particles are mediated by transmembrane ATP binding cassette transporter A1 (ABCA1) (*5*). Subsequently, apoA-I in these HDL particles acts as a cofactor for lecithin:cholesterol acyltransferase (LCAT) to convert cholesterol to cholesteryl ester (*6*). Finally, esterified cholesterol in mature HDL particles is selectively delivered to hepatocytes via scavenger receptor class B type I (SR-BI) without uptake of entire particles; apoA-I is the preferred ligand for SR-BI (*7*).

Human apoA-I is a 243-amino acid residue protein that is composed of 11- or 22-amino acid tandem repeats, which can form amphipathic α-helices, punctuated by proline residues (*8*, *9*). In the lipid-free state, apoA-I-like apoE is postulated to have two structural domains: an α-helix bundle that is formed by the N-terminal and central regions and a less organized domain formed by the C-terminal region (*10*, *11*). It is proposed that interaction of apoA-I with lipid initially occurs through the C-terminal domain followed by an opening of the N-terminal helix bundle (*10*, *11*). Amphipathic α-helices are the structural motif known to facilitate the binding of apolipoproteins to lipids (*8*, *9*). Exchangeable apolipoproteins with multiple amphipathic helices have been shown to efflux lipid from ABCA1-transfected cells, indicating that lipid efflux is not specific for apoA-I (*12*). Even synthetic amphipathic helical peptides are able to promote lipid efflux from cell (*13*). On the other hand, deletion or disruption of the C-terminal region of the apoA-I molecule reduces ABCA1-mediated lipid efflux in a major fashion (*14*, *15*). Although the detailed mechanism for ABCA1-mediated lipid efflux is unknown at this time, it is likely that interaction of α-helical segments in apolipoproteins with the plasma membrane is a critical factor for lipid release from the cell surface. During lipoprotein metabolism in plasma, apoA-I

† This work was supported by NIH Grant HL22633.

* To whom correspondence should be addressed: Abramson Research Center, The Children's Hospital of Philadelphia, Suite 1102, 3615 Civic Center Blvd., Philadelphia, PA 19104-4318. Telephone: (215) 590-0587. Fax: (215) 590-0583. E-mail: Phillipsmi@email.chop.edu.

‡ University of Pennsylvania School of Medicine.

§ Current address: Kobe Pharmaceutical University, 4-19-1 Motoyama-kitamachi, Higashinada-ku, Kobe 658-8558, Japan.

‖ Kyoto University.

[1] Abbreviations: Apo, apolipoprotein; CD, circular dichroism; HDL, high-density lipoprotein; ITC, isothermal titration calorimetry; LEM, large emulsion; LUV, large unilamellar vesicles; NMR, nuclear magnetic resonance; PC, phosphatidylcholine; SEM, small emulsion; SUV, small unilamellar vesicles; TO, triolein; WT, wild-type.

10.1021/bi050853+ CCC: $30.25
Published on Web 07/13/2005

cycles between lipid-free and lipid-bound forms, changing its structural organization depending on the size and the phospholipid composition of the lipoprotein particles with which it is associated (*16*). Such structural flexibility underlies the multiple functions of this protein.

Previously, we showed that α-helix formation enthalpically drives apoA-I to bind to egg phosphatidylcholine (PC) small unilamellar vesicles (SUV) with high affinity (*17*). However, differences in surface curvature and composition of lipid particles modify the membrane properties and therefore affect the binding of exchangeable apolipoproteins. For example, addition of cholesterol to a phospholipid bilayer membrane increases the level of apoA-I and model α-helical peptide binding (*18*, *19*). Phospholipid bilayer vesicles are commonly used as a cell membrane model, whereas lipid emulsion droplets composed of a triglyceride (TG) core covered by a phospholipid monolayer are model particles for TG-rich lipoprotein. In this study, we investigated the energetics of binding of apoA-I to model lipoprotein particles with a TG core, using centrifugation, calorimetry, circular dichroism (CD), and nuclear magnetic resonance (NMR) techniques.

MATERIALS AND METHODS

Materials. Egg PC and triolein (TO) were purchased from Sigma. [^{14}C]Formaldehyde was purchased from PerkinElmer Life Sciences. Plasma apoA-I was isolated from human HDL as described previously (*20*). Wild-type (WT) human apoA-I and engineered deletion mutants were expressed as thioredoxin fusion proteins in *Escherichia coli* strain BL21-DE3 and then cleaved and purified as described previously (*10*). The apoA-I preparations were at least 95% pure as assessed by SDS−PAGE. In all experiments, apoA-I was freshly dialyzed at concentrations of ≤1 mg/mL from a 6 M guanidine hydrochloride solution into the appropriate buffer before use.

Preparation of Large and Small Emulsion Particles. Homogeneous emulsion particles composed of egg PC and TO were prepared in Tris buffer [10 mM Tris-HCl, 150 mM NaCl, 0.02% NaN_3, and 1 mM EDTA (pH 7.4)] by sonication and separated from phospholipid vesicles by ultracentrifugation as described previously (*21*). Egg PC and TO concentrations were determined using enzymatic assay kits from Wako (Richmond, VA). The average particle diameters determined by quasi-elastic light scattering measurements were 120 ± 10 and 35 ± 5 nm for LEM and SEM, respectively. TO/PC molar ratios were ∼6 and ∼2 for LEM and SEM, respectively. The emulsions were stored under nitrogen at room temperature and used within 2 weeks.

Binding of ApoA-I to Emulsion Particles. Binding of WT and mutant forms of apoA-I to emulsion particles was assayed by a centrifugation method (*21*). Trace amounts of ^{14}C label were introduced into the apoA-I preparations by reductive methylation of lysines with [^{14}C]formaldehyde as described previously (*22*). In this modification, there is no detectable change in the physical properties of the protein. The mixtures of a constant amount of emulsion and various amounts of ^{14}C-labeled apoA-I were incubated for 1 h at room temperature. After incubation, the mixtures were centrifuged at 30 000 (for LEM) or 50 000 rpm (for SEM) in a Beckman 50Ti rotor for 30 min to separate the bound protein (the top fraction) from the free protein (the bottom fraction). The radioactivity in the top and bottom fractions was quantitated by liquid scintillation counting. The bound apoA-I concentration was calculated by subtracting the background free apoA-I concentration in the top fraction; the latter was obtained from the results of centrifugation of lipid-free apoA-I solutions. Binding data were fitted by nonlinear regression to a one-binding site model with GraphPad Prism. The dissociation constant, K_d, and binding maximum, B_{max}, were determined as the fitting parameters.

Isothermal Titration Calorimetry (ITC) Measurements. Heats generated by binding of apoA-I to lipid particles were monitored using a MicroCal MCS isothermal titration calorimeter at 25 °C, as described previously (*10*, *21*). All solutions were degassed under vacuum before use. Lipid particles (15 mM PC) were placed into the sample cell (1.35 mL) and titrated with 8 μL aliquots of the apoA-I sample (0.8 mg/mL) with continual stirring at 400 rpm. The heat of dilution of apoA-I was subtracted from the corresponding heats of mixing.

CD Spectroscopy. CD measurements were performed at room temperature using a Jasco J-600 spectropolarimeter calibrated with ammonium *d*-(+)-10-camphorsulfonate. ApoA-I samples were dissolved at 25 μg/mL in 10 mM sodium phosphate buffer (pH 7.4) and measured in a 1 mm path length quartz cell to prevent light scattering due to the presence of lipid particles. For the apoA-I/lipid mixture samples, apoA-I was incubated with lipid particles for 1 h prior to the measurement. Eight to ten scans were averaged for each sample. The results were corrected by subtracting the buffer baseline or a blank sample containing an identical concentration of lipid. The α-helix contents were calculated from the equation

$$\%\ \alpha\text{-helix} = ([\theta]_{222} + 3000)/39000$$

where $[\theta]_{222} = (\mathrm{MRW})\theta_{222}/10lc$, θ_{222} is the measured ellipticity in degrees at 222 nm, l is the cuvette path length in centimeters, and c is the protein concentration in grams per milliliter. A mean residue weight (MRW) was obtained from the molecular weight and the number of amino acids.

NMR Measurements. ^{13}C NMR spectra of LEM and SEM in 10 mM sodium phosphate buffer (pH 7.4) were obtained with a Bruker Avance DMX400 spectrometer equipped with a 10 mm triple probe. A 1 mL microcell containing the emulsion sample was introduced into the 10 mm tube containing D_2O for the lock. The sample temperature was set at 37 °C. The spectra were recorded using a 45° pulse with proton decoupling. The acquisition conditions were as follows: a spectral width of 25 kHz, 64K data points, an acquisition time of 1.3 s, 128 dummy scans, and a relaxation delay of 0.1 s; 40000−160000 free induction decays were accumulated. An aqueous solution of dioxane in a sealed capillary was used as the external reference. All spectra were processed with 3.0 Hz exponential filtering.

RESULTS

Binding of ApoA-I to Emulsion Particles. To investigate the role of various domains of apoA-I in lipid binding, we examined the binding of apoA-I deletion/point mutants to lipid emulsions as model lipoprotein particles. Panels a and b of Figure 1 show the isotherms for binding of WT apoA-I, deletion mutants, and proline substitution mutants to LEM.

Table 1: Parameters for Binding of ApoA-I to Lipid Emulsions[a]

	35 nm emulsion (SEM)		120 nm emulsion (LEM)	
	K_d (μg/mL)	B_{max} (no. of amino acids/mol of PC)	K_d (μg/mL)	B_{max} (no. of amino acids/mol of PC)
plasma	5.0 ± 1.7	0.21 ± 0.02	18.9 ± 10.1	0.17 ± 0.03
WT	7.5 ± 1.6	0.21 ± 0.01	23.9 ± 5.6	0.18 ± 0.02
Δ1−43	2.9 ± 0.4	0.17 ± 0.00	12.4 ± 4.1	0.12 ± 0.01
Δ44−65	6.3 ± 1.0	0.13 ± 0.00[b]	12.6 ± 4.6	0.06 ± 0.02[b]
Δ44−126	4.5 ± 1.1	0.27 ± 0.01[b]	8.4 ± 2.7	0.16 ± 0.01
Δ123−166	1.9 ± 0.5	0.19 ± 0.01	9.8 ± 2.7	0.14 ± 0.01
Δ190−243	8.7 ± 5.1	0.03 ± 0.00[b]	20.4 ± 8.4	0.03 ± 0.01[b]
Δ223−243	18.2 ± 5.1	0.09 ± 0.01[b]	39.4 ± 25.8	0.04 ± 0.01[b]
L230P	5.1 ± 1.9	0.08 ± 0.01[b]	12.9 ± 5.3	0.04 ± 0.01[b]
L230P/L233P/Y236P	8.7 ± 3.1	0.08 ± 0.01[b]	18.3 ± 8.0	0.05 ± 0.01[b]

[a] All data represent the mean ± the standard error of at least two independent experiments each performed in duplicate. [b] $P < 0.01$ compared to WT.

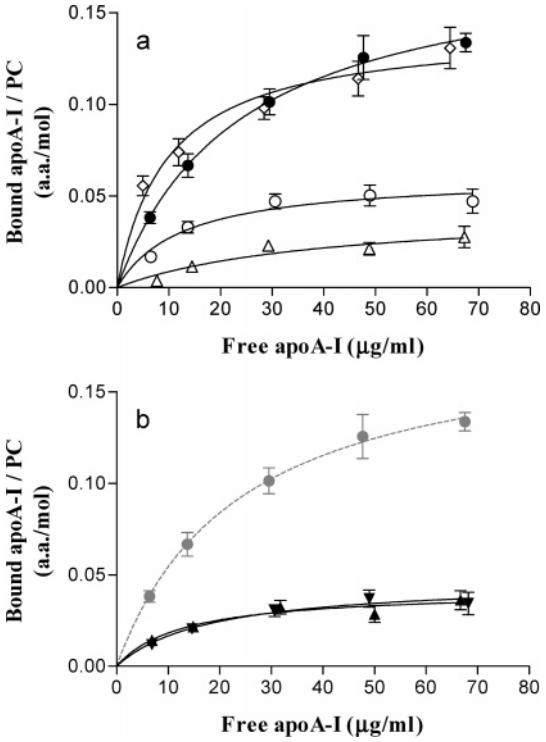

FIGURE 1: Isotherms for binding of apoA-I variants to LEM: (a) WT apoA-I (●), Δ44−65 (○) Δ123−166 (◇), and Δ223−243 (△) and (b) WT apoA-I (●), L230P (▲), and L230P/L236P/Y236P (▼). The binding curves were obtained by nonlinear regression fitting to a one-binding site model.

The binding parameters are summarized in Table 1. B_{max} values indicate the extent to which the protein occupies the surface area and therefore provide insight into the protein conformation on the particle. Notably, B_{max} for WT apoA-I (~0.2 amino acid/mol of PC) is smaller than that for apoE (~0.8 amino acid/mol of PC) (*21*), meaning that one apoA-I molecule occupies more surface area than apoE. This probably arises because more helices in apoA-I are in contact with the lipid surface; some helices of apoE remain out of contact with the lipid in the lipid-bound state (*21*).

Compared to WT apoA-I, deletion of the C-terminal region (Δ223−243 and Δ190−243) decreased B_{max} significantly and increased K_d somewhat. Also, deletion of the N-terminal region (Δ1−43 and Δ44−65) decreased the B_{max}. On the other hand, deletion of the central region (Δ123−166) did not change the B_{max} of apoA-I. It is well-known that insertion of a proline residue into a protein sequence disrupts the α-helix conformation (*23*). Proline residues were incorporated into the C-terminal domain spanning residues 223−243 which is very hydrophobic as judged from hydropathy analysis of the amino acid sequence of apoA-I (*11*). Anticipating that substitution of a single amino acid (L230) with proline may not be sufficient to disrupt the α-helix conformation, we also substituted three amino acids (L230, L233, and Y236) with proline residues. CD measurements (data not shown) indicated that both mutants exhibited the same decrease in α-helix content as the Δ223−243 mutant when compared to WT apoA-I. The L230P and L230P/L233P/Y236P mutations both markedly decreased B_{max} (Figure 1b) in a manner similar to that of the corresponding C-terminal deletion mutants.

The effect of particle size on apoA-I binding was also examined. LEM and SEM particles are homogeneous and significantly different in size from each other. In all mutants that were studied, apoA-I exhibited 2−3 times higher affinity (smaller K_d value) for SEM than for LEM (Table 1). However, the B_{max} of WT apoA-I was comparable for both particles (0.21 and 0.18 amino acid/mol of PC for SEM and LEM, respectively), suggesting that the overall apoA-I organization on these particles is similar.

Calorimetric Measurements. ITC measurements were carried out to obtain the thermodynamic parameters characterizing the binding of apoA-I to lipid particles. The lipid to protein concentration ratio was high enough to ensure the complete binding of the injected proteins. Panels a and b of Figure 2 compare the isothermal titration curves of WT apoA-I and its proline mutant (L230P) injected into LEM, SEM, and buffer. The initial tiny exothermic peak shown in the injection into SEM represents the dilution heat of apoA-I. Dilution heats obtained from the titration of apoA-I into buffer were subtracted from the heat of mixing. Integration of the peak yielded the binding enthalpies (ΔH) (Table 2). The free energies (ΔG) and entropies of binding (ΔS) were calculated using the binding constant (K_d) given in Table 1 (Table 2). The enthalpies of binding of apoA-I to LEM and SUV were similar (*10*, *17*); the binding of WT apoA-I was accompanied by a large exothermic heat that was markedly reduced for the C-terminal deletion mutants. In addition, insertion of proline residues into the C-terminal region significantly decreased the enthalpy of binding to LEM (Figure 2b) and SUV (data not shown). This observation indicates that disruption of the α-helix conformation in the C-terminal domain weakened the ability of apoA-I to bind

Table 2: Thermodynamic Parameters for Binding of Apo-I to Lipid Emulsions[a]

	SEM			LEM		
	ΔH (kcal/mol)	ΔG[b] (kcal/mol)	ΔS[c] (cal mol^{-1} K^{-1})	ΔH (kcal/mol)	ΔG (kcal/mol)	ΔS
plasma	29.0 ± 1.2	−11.5 ± 0.2	136 ± 5	−84.2 ± 3.4[d]	−10.7 ± 0.3	−247 ± 12
WT	29.5 ± 1.7	−11.3 ± 0.1	137 ± 6	−85.5 ± 3.6[d]	−10.6 ± 0.1	−251 ± 12
Δ1−43	7.0 ± 2.7	−11.8 ± 0.1	63 ± 9	−20.5 ± 2.9[d]	−10.9 ± 0.2	−32 ± 10
Δ44−65	17.0 ± 4.0	−11.4 ± 0.1	95 ± 14	−76.3 ± 3.4[d]	−10.9 ± 0.2	−219 ± 12
Δ44−126	−5.0 ± 0.5	−11.4 ± 0.1	21 ± 2	−63.1 ± 3.2[d]	−11.0 ± 0.2	−175 ± 11
Δ123−166	11.5 ± 1.6	−12.0 ± 0.1	79 ± 6	−72.3 ± 2.1[d]	−11.0 ± 0.1	−206 ± 7
Δ190−243	4.0 ± 0.9	−11.1 ± 0.3	51 ± 4	−18.5 ± 2.1[d]	−10.6 ± 0.2	−26 ± 8
Δ223−243	0.8 ± 3.3	−10.7 ± 0.1	39 ± 11	−21.5 ± 3.5[d]	−10.3 ± 0.3	−38 ± 13
L230P	10.8 ± 3.4	−11.5 ± 0.2	75 ± 12	−30.3 ± 4.7	−11.0 ± 0.2	−65 ± 16
L230P/L233P/Y236P	1.5 ± 2.5	−11.2 ± 0.2	43 ± 9	−14.7 ± 2.4	−10.8 ± 0.2	−13 ± 9

[a] Mean ± the standard deviation ($n = 4$). [b] The free energy was calculated according to $\Delta G = -RT \ln 55.5(1/K_d)$ using the binding constants given in Table 1. [c] The entropy of binding was calculated from $\Delta G = \Delta H - T\Delta S$. [d] From ref 10.

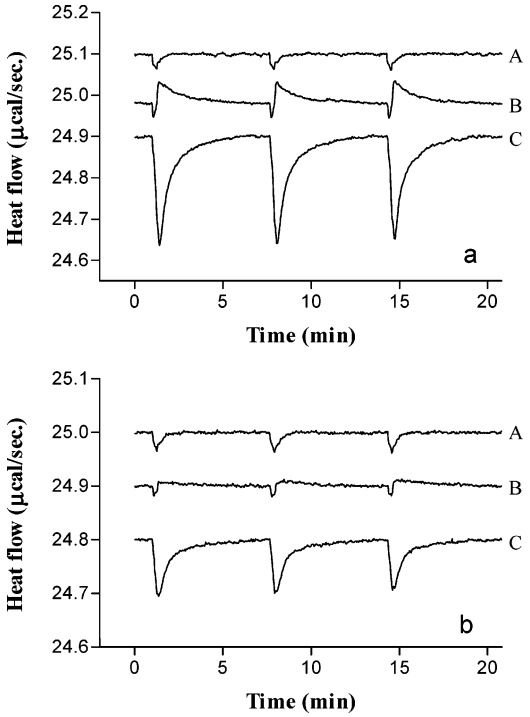

FIGURE 2: Isothermal titration calorimetry of WT apoA-I (a) and L230P (b) injected into Tris-buffer (A), SEM (B), and LEM (C). Lipid particles (15 mM PC) were placed into the sample cell (1.35 mL) and titrated with 8 μL aliquots of the apoA-I sample (0.8 mg/mL) with continual stirring at 400 rpm. The heats generated upon binding of apoA-I to emulsions were calculated by subtracting the dilution heat of the protein (A).

to lipid, consistent with the direct binding measurements (Figure 1). In marked contrast, the heat of binding of apoA-I to SEM was endothermic as shown in Figure 2 and summarized in Table 2. This result indicates that binding of apoA-I to SEM is an enthalpically unfavorable process. A similar phenomenon was observed in the binding of apoE, where the apoE binding to SEM was much less exothermic than that to LEM (*21*). Given that apoA-I has a much higher affinity for SEM than for LEM (Table 1), the entropic contribution overwhelms the unfavorable enthalpic contribution in binding of apoA-I to SEM.

Correlation of Thermodynamic Parameters of ApoA-I Binding with α-Helix Formation. The fact that the binding of apoA-I to SEM is an endothermic process suggests that there would be little or no increase in α-helix content when apoA-I binds to SEM, because α-helix formation is supposed to generate exothermic heat (−1.1 kcal/α-helical residue)

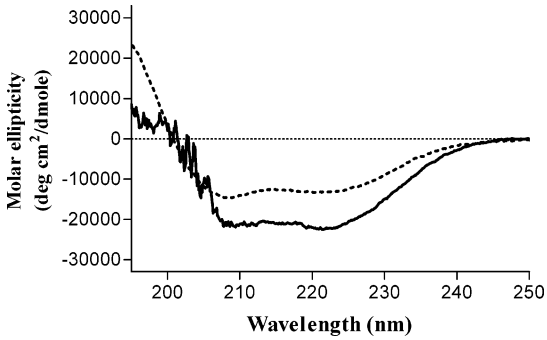

FIGURE 3: Far-UV CD spectra of WT apoA-I in the absence (- - -) and presence (—) of SEM. The concentration of apoA-I was 25 μg/mL. In the mixture of apoA-I and SEM, the PC to apoA-I weight ratio was set to 40:1.

upon binding to lipid (*17*). To address this issue, far-UV CD measurements were performed in the absence and presence of excess SEM. Under these conditions, almost all the apoA-I molecules were bound to SEM as deduced from the binding isotherms. The CD spectra of samples containing SEM were slightly noisy due to some light scattering, but at 222 nm, the effect was negligible (Figure 3). CD measurements with LEM were not possible because of excessive light scattering. The increase in α-helix content of WT apoA-I upon binding to SEM and SUV was similar (~25%).

The thermodynamic parameters of apoA-I binding are represented as a function of the increase in the number of α-helical residues upon binding to SEM in Figure 4. In contrast to the binding to SUV elucidated in a previous study (*17*), the plot of binding enthalpy versus the increase in α-helical residues shows a positive slope for SEM (Figure 4), suggesting that α-helix formation does not enthalpically drive apoA-I to bind to SEM. Interestingly, although the slopes for the SEM and SUV plots are opposite, the nonhelical contribution to the enthalpy (*Y*-intercept) was similar ($\Delta H_0 \sim -20$ kcal/mol) in both cases. This result implies that the binding that occurs without any changes in α-helix content is not affected by the presence of a TG core in the SEM particles. The free energies of binding of the apoA-I variant to SEM were relatively constant, and there seems to be no correlation with the increase in the number of α-helical residues (inset of Figure 4). It follows that the binding of apoA-I to SEM is an entropy-driven process in contrast to an enthalpy-driven process with SUV. Assuming that all amino acid residues that converted from random coil to α-helix contribute to the enthalpy of binding, the ΔH value

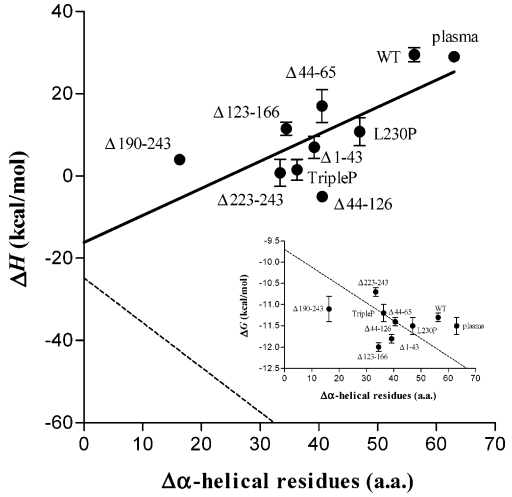

FIGURE 4: Correlation of the binding enthalpy and free energy (inset) with the increase in the number of α-helical residues upon binding of apoA-I to SEM. The solid line represents the best-fit regression line ($r^2 = 0.53$). No significant correlation was observed in the equivalent binding free energy plot. Dashed lines represent the regression lines obtained with binding of apoA-I to SUV (*17*). TripleP represents the L230P/L233P/Y236P mutant.

Table 3: Chemical Shifts for Selected PC and TO Resonances from Lipid Emulsions[a]

	chemical shift (ppm)[b]	
	SEM	LEM
PC		
$N(CH_3)_3$	53.68	53.67
CH_2N	65.67	65.65
CH_2OP	59.06	59.05
C═O (sn-2)	173.12	173.10
C═O (sn-1)	172.97	172.98
TO		
C═O (sn-1,3)	171.13	171.13
C═O (sn-2)	170.84	170.85

[a] Dioxane in capillary was used for the chemical shift reference set at 66.7 ppm. [b] Experimental errors were ±0.02 ppm for the chemical shifts.

is expected to be −62 kcal/mol for binding of WT apoA-I to SEM (−1.1 kcal/α-helical residue multiplied by 56 amino acids). The difference between the estimated and measured values is ∼90 kcal/mol. The presence of the core lipid in SEM seems to cancel out the exothermic heat induced by apoA-I α-helix formation. Seelig et al. (*24*) suggested that the contribution of α-helix formation to the thermodynamics of binding is not influenced by the curvature of lipid particles. In light of this finding, although the increase in α-helix content upon apoA-I binding to LEM is unknown, it is likely that such compensation of the heat does not occur in binding of apoA-I to LEM. It follows that some unique event(s) accompanies apoA-I α-helix formation at the SEM surface.

^{13}C NMR Measurements of Lipid Emulsions. To compare the packing of lipid molecules in LEM and SEM, ^{13}C NMR measurements were performed. Several resonances were explicitly resolved and found to be specific for either PC or TO. For example, two distinct PC carbonyl resonances originating from the sn-1 and sn-2 PC acyl chains were observed (Table 3). Other resonances derived especially from acyl chain carbons could not be resolved successfully. Comparison of chemical shifts (Table 3) revealed that there is no significant difference in the polarity of the PC molecule environment in LEM and SEM.

DISCUSSION

The aim of this study is to gain insight into the binding of apoA-I to lipid emulsions as model lipoprotein particles. Previously, we proposed that apoA-I is composed of two structural domains in the lipid-free state: an α-helix bundle of N-terminal and central domains and a less organized C-terminal domain (*10*, *11*). Initial lipid binding occurs through the C-terminal domain triggering α-helix formation in other regions of apoA-I. Such α-helix formation enthalpically drives apoA-I to bind to the phospholipid bilayer in SUV (*17*). It has been shown that the presence of the core lipid in emulsion particles modifies the properties of the particle phospholipid surface (*26*), but the consequences for apoA-I binding are not known. Here, we explored the effects of the core lipid on the energetics of binding of apoA-I to phospholipid-stabilized emulsion droplets.

Contributions of Different ApoA-I Domains to Binding to Lipid Emulsions. Consistent with prior investigations, this study indicated that the extreme C-terminal domain (residues 223−243) of apoA-I is critical for lipid binding (*17*, *27*). Also, the decreased level of binding of the Δ44−65 mutant is consistent with the result that two terminal 22-mer (44−65 and 220−241) peptides strongly interact with lipid (*28*, *29*). Residues 223−243 are apparently α-helical in the lipid-free state (*30*). Insertion of proline residues into this region (L230P and L230P/L233P/Y236P) to prevent α-helix formation significantly decreased the level of binding as much as that seen with the Δ223−243 mutant. Furthermore, the heat generated upon binding of apoA-I to LEM or SUV was largely decreased by the proline insertion (Table 2). These results indicated that the α-helix conformation in this domain plays a critical role in initial lipid binding.

Deletion of the central region (Δ123−166) did not change B_{max} or the enthalpy of binding to lipid emulsions, implying that this region is not involved in lipid binding. Recently, it has been proposed that some of the central regions of apoA-I, depending upon the surface pressure, detach from the TO−water interface with the N- and C-terminal domains remaining attached (*31*). It may be inferred that this central region is out of contact with the surface on emulsion particles.

Although residues 1−44 contain a highly hydrophobic segment, as judged from hydropathy plots (*11*), the peptide corresponding to residues 1−44 is unstructured in aqueous solution (*32*). In the intact apoA-I molecule, the N- and C-terminal domains are considered to interact with each other and contribute to the stabilization of the overall protein structure (*33*). Binding experiments showed that the Δ1−43 mutation decreased B_{max} somewhat (Table 1). This result may arise because the deletion of the N-terminal domain disrupts the hypothetical N- and C-terminal domain interaction, leading to unfolding of the α-helix in the C-terminal domain (*33*).

Surface Properties of Lipid Emulsions and ApoA-I Binding. SEM with an average diameter of 35 nm is characterized by a highly curved surface, whereas LEM with an average diameter of 120 nm forms a relatively flat surface in terms of phospholipid molecular packing. The structural organization of apoA-I α-helices on a spherical particle surface is

not known, but the amphipathic α-helices are thought to intercalate between PC molecules with the hydrophobic face embedded between the PC acyl chains (*34*). ApoA-I recognizes headgroup separation (hydrated space) between PC molecules and displaces water molecules from the surface when it binds (*18*, *26*, *35*).

The surface of an SUV is much more hydrated than that of a large unilamellar vesicle (LUV) because of the differences in curvature (*26*). In contrast, no differences were observed in the lipid chemical shifts for LEM and SEM (Table 3), which indicates that the polarity (i.e., degree of hydration) in the phospholipid surface is the same in both particles despite the differences in curvature. Interpenetration of core TO molecules with phospholipid molecules in the surface monolayer occurs in emulsion particles (*26*, *36*). Apparently, these TO molecules compensate for the greater hydrated space between PC molecules in SEM that would otherwise arise from the greater surface curvature so that the polarities of the LEM and SEM surfaces are the same.

Previously, we showed that the highly curved surface structure of SUV led to a marked increase in the B_{max} of apoA-I compared to the relatively flat surface of LUV (*26*). In the study presented here, on the other hand, B_{max} is similar for LEM and SEM. This result is consistent with the previous observations that the degree of binding of apoA-I to lipid particles is modulated by the degree of hydration in the PC carbonyl region (*26*). Although the lipid constituents are identical, apoA-I exhibited 2−3 times higher affinity for SEM than for LEM (Table 1); a similar effect of particle size was observed for binding of apoA-I to SUV and LUV (*26*). The reasons for this effect are not entirely clear but perhaps arise because the α-helical segments in apoA-I are more deeply embedded into the SEM surface than into the LEM surface. In support of this concept, it has been shown that the presence of cholesterol in a phospholipid bilayer, which tightens the membrane packing, reduces both the depth of penetration and the binding affinity of an α-helical peptide (*19*, *37*).

Contribution of the Core Lipid to the Energetics of ApoA-I Binding. The transition from random coil to α-helix has been shown to produce a large negative enthalpy (exothermic heat) that drives lipid binding (*17*, *38*−*40*). However, the heat generated upon binding of apoA-I to SEM was endothermic regardless of the fact that apoA-I increased its α-helix content. What are the sources of the 90 kcal/mol change in ΔH and the change in sign of ΔS in binding of WT apoA-I to SEM as compared to SUV and LEM? There are several other possible factors that could contribute to the thermodynamics of lipid binding. Formation of noncovalent bonds occurs in protein−lipid interactions. In the case of binding of apoA-I to SEM, the nonpolar face of amphiphathic α-helices interacts with PC acyl chains through hydrophobic interactions. Also, there can be electrostatic interactions between the negatively charged phosphate group of PC molecules and positively charged amino acid side chains in apoA-I (*34*). These interactions are expected to generate exothermic heat. The binding of apoA-I to the emulsion surface expels water molecules from the membrane interface, and the release of ordered water molecules gives rise to positive enthalpy and entropy changes (*35*). When the fact that both the degree of hydration and the amount of bound apoA-I are similar for LEM and SEM is taken into account, there is not likely to be much difference in the effect of dehydration on the thermodynamic parameters characterizing binding of apoA-I to these particles. The lateral compressibility of a lipid membrane is an important determinant of the thermodynamics of lipid−protein interaction, and in the case of LUV, penetration of an α-helical peptide disorders the PC acyl chains so that both the enthalpy and entropy of binding are positive (*41*). Positive changes in enthalpy and entropy also occur when apoA-I binds to SEM (Table 2), suggesting that similar changes in the particle surface occur in this case. It is possible that the relatively deep penetration of apoA-I into the SEM surface mentioned in the preceding section induces the separation of PC acyl chains, giving rise to an endothermic heat in a manner similar to acyl chain melting (*35*, *42*). Also, such deeper apoA-I penetration may displace TO molecules from among the PC acyl chains into the bulk TO particle core. Such weakened interaction between the acyl chains of PC and TO should lead to increases in enthalpy and entropy. Relatively minor perturbation of the surface occurs when apoA-I binds to SUV, where the PC molecules are relatively loosely packed; the heat generated from α-helix formation dominates the thermodynamic process (*17*).

In summary, apoA-I can bind with relatively high affinity ($K_d \sim 10^{-7}$ M) to curved phospholipid bilayer surfaces and to microemulsion particle surfaces. Enthalpic α-helix formation drives binding of apoA-I to SUV (25 nm diameter), whereas binding to emulsion droplets (35 nm diameter) is entropically driven. The quite different energetics of lipid−protein interaction in the model lipoprotein particle are proposed to arise because the presence of TO molecules alters the surface structure, allowing deeper apoA-I α-helix penetration and more perturbation of surface lipid acyl chain packing.

ACKNOWLEDGMENT

We thank Drs. Saburo Aimoto and Toru Kawakami (Institute for Protein Research, Osaka University, Osaka, Japan) for their help with ITC measurements.

REFERENCES

1. Gordon, T., Castelli, W. P., Hjortland, M. C., Kannel, W. B., and Dawber, T. R. (1977) High-density lipoprotein as a protective factor against coronary heart disease. The Framingham Study, *Am. J. Med. 62*, 707−714.
2. von Eckardstein, A., Nofer, J. R., and Assmann, G. (2001) High-density lipoproteins and arteriosclerosis. Role of cholesterol efflux and reverse cholesterol transport, *Arterioscler. Thromb. Vasc. Biol. 21*, 13−27.
3. Fielding, C. J., and Fielding, P. E. (1995) Molecular physiology of reverse cholesterol transport, *J. Lipid Res. 36*, 211−228.
4. Yokoyama, S. (1998) Apolipoprotein-mediated cellular cholesterol efflux, *Biochim. Biophys. Acta 1392*, 1−15.
5. Oram, J. F. (2003) HDL apolipoproteins and ABCA1: Partners in the removal of excess cellular cholesterol, *Arterioscler. Thromb. Vasc. Biol. 23*, 720−727.
6. Jonas, A. (1991) Lecithin-cholesterol acyltransferase in the metabolism of high-density lipoproteins, *Biochim. Biophys. Acta 1084*, 205−220.
7. Krieger, M. (2001) Scavenger receptor class B type I is a multiligand HDL receptor that influences diverse physiologic systems, *J. Clin. Invest. 108*, 793−797.
8. Segrest, J. P., Jones, M. K., De Loof, H., Brouillette, C. G., Venkatachalapathi, Y. V., and Anantharamaiah, G. M. (1992) The amphipathic helix in the exchangeable apolipoproteins: A review of secondary structure and function, *J. Lipid Res. 33*, 141−166.

9. Frank, P. G., and Marcel, Y. L. (2000) Apolipoprotein A-I: Structure−function relationships, *J. Lipid Res. 41*, 853−872.
10. Saito, H., Dhanasekaran, P., Nguyen, D., Holvoet, P., Lund-Katz, S., and Phillips, M. C. (2003) Domain structure and lipid interaction in human apolipoproteins A-I and E, a general model, *J. Biol. Chem. 278*, 23227−23232.
11. Saito, H., Lund-Katz, S., and Phillips, M. C. (2004) Contributions of domain structure and lipid interaction to the functionality of exchangeable human apolipoproteins, *Prog. Lipid Res. 43*, 350−380.
12. Remaley, A. T., Stonik, J. A., Demosky, S. J., Neufeld, E. B., Bocharov, A. V., Vishnyakova, T. G., Eggerman, T. L., Patterson, A. P., Duverger, N. J., Santamarina-Fojo, S., and Brewer, H. B., Jr. (2001) Apolipoprotein specificity for lipid efflux by the human ABCAI transporter, *Biochem. Biophys. Res. Commun. 280*, 818−823.
13. Remaley, A. T., Thomas, F., Stonik, J. A., Demosky, S. J., Bark, S. E., Neufeld, E. B., Bocharov, A. V., Vishnyakova, T. G., Patterson, A. P., Eggerman, T. L., Santamarina-Fojo, S., and Brewer, H. B. (2003) Synthetic amphipathic helical peptides promote lipid efflux from cells by an ABCA1-dependent and an ABCA1-independent pathway, *J. Lipid Res. 44*, 828−836.
14. Panagotopulos, S. E., Witting, S. R., Horace, E. M., Hui, D. Y., Maiorano, J. N., and Davidson, W. S. (2002) The role of apolipoprotein A-I helix 10 in apolipoprotein-mediated cholesterol efflux via the ATP-binding cassette transporter ABCA1, *J. Biol. Chem. 277*, 39477−39484.
15. Vedhachalam, C., Liu, L., Nickel, M., Dhanasekaran, P., Anantharamaiah, G. M., Lund-Katz, S., Rothblat, G. H., and Phillips, M. C. (2004) Influence of apoA-I structure on the ABCA1-mediated efflux of cellular lipids, *J. Biol. Chem. 279*, 49931−49939.
16. Rye, K. A., and Barter, P. J. (2004) Formation and metabolism of pre-β-migrating, lipid-poor apolipoprotein A-I, *Arterioscler. Thromb. Vasc. Biol. 24*, 421−428.
17. Saito, H., Dhanasekaran, P., Nguyen, D., Deridder, E., Holvoet, P., Lund-Katz, S., and Phillips, M. C. (2004) α-Helix formation is required for high affinity binding of human apolipoprotein A-I to lipids, *J. Biol. Chem. 279*, 20974−20981.
18. Saito, H., Miyako, Y., Handa, T., and Miyajima, K. (1997) Effect of cholesterol on apolipoprotein A-I binding to lipid bilayers and emulsions, *J. Lipid Res. 38*, 287−294.
19. Egashira, M., Gorbenko, G., Tanaka, M., Saito, H., Molotkovsky, J., Nakano, M., and Handa, T. (2002) Cholesterol modulates interaction between an amphipathic class A peptide, Ac-18A-NH_2, and phosphatidylcholine bilayers, *Biochemistry 41*, 4165−4172.
20. Gillotte, K. L., Zaiou, M., Lund-Katz, S., Anantharamaiah, G. M., Holvoet, P., Dhoest, A., Palgunachari, M. N., Segrest, J. P., Weisgraber, K. H., Rothblat, G. H., and Phillips, M. C. (1999) Apolipoprotein-mediated plasma membrane microsolubilization. Role of lipid affinity and membrane penetration in the efflux of cellular cholesterol and phospholipids, *J. Biol. Chem. 274*, 2021−2028.
21. Saito, H., Dhanasekaran, P., Baldwin, F., Weisgraber, K. H., Lund-Katz, S., and Phillips, M. C. (2001) Lipid binding-induced conformational change in human apolipoprotein E. Evidence for two lipid-bound states on spherical particles, *J. Biol. Chem. 276*, 40949−40954.
22. Lund-Katz, S., Weisgraber, K. H., Mahley, R. W., and Phillips, M. C. (1993) Conformation of apolipoprotein E in lipoproteins, *J. Biol. Chem. 268*, 23008−23015.
23. Barlow, D. J., and Thornton, J. M. (1988) Helix geometry in proteins, *J. Mol. Biol. 201*, 601−619.
24. Wieprecht, T., Beyermann, M., and Seelig, J. (2002) Thermodynamics of the coil-α-helix transition of amphipathic peptides in a membrane environment: The role of vesicle curvature, *Biophys. Chem. 96*, 191−201.
25. Schmidt, C. F., Barenholz, Y., Huang, C., and Thompson, T. E. (1977) Phosphatidylcholine ^{13}C-labeled carbonyls as a probe of bilayer structure, *Biochemistry 16*, 3948−3954.
26. Saito, H., Tanaka, M., Okamura, E., Kimura, T., Nakahara, M., and Handa, T. (2001) Interactions of phosphatidylcholine surface monolayers with triglyceride cores and enhanced apoA-1 binding in lipid emulsions, *Langmuir 17*, 2528−2532.
27. Davidson, W. S., Hazlett, T., Mantulin, W. W., and Jonas, A. (1996) The role of apolipoprotein AI domains in lipid binding, *Proc. Natl. Acad. Sci. U.S.A. 93*, 13605−13610.
28. Palgunachari, M. N., Mishra, V. K., Lund-Katz, S., Phillips, M. C., Adeyeye, S. O., Alluri, S., Anantharamaiah, G. M., and Segrest, J. P. (1996) Only the two end helixes of eight tandem amphipathic helical domains of human apo A-I have significant lipid affinity. Implications for HDL assembly, *Arterioscler. Thromb. Vasc. Biol. 16*, 328−338.
29. Mishra, V. K., Palgunachari, M. N., Datta, G., Phillips, M. C., Lund-Katz, S., Adeyeye, S. O., Segrest, J. P., and Anantharamaiah, G. M. (1998) Studies of synthetic peptides of human apolipoprotein A-I containing tandem amphipathic α-helixes, *Biochemistry 37*, 10313−10324.
30. Oda, M. N., Forte, T. M., Ryan, R. O., and Voss, J. C. (2003) The C-terminal domain of apolipoprotein A-I contains a lipid-sensitive conformational trigger, *Nat. Struct. Biol. 10*, 455−460.
31. Wang, L., Atkinson, D., and Small, D. M. (2005) The interfacial properties of apoA-I and an amphipathic α-helix consensus peptide of exchangeable apolipoproteins at the triolein/water interface, *J. Biol. Chem. 280*, 4154−4165.
32. Zhu, H. L., and Atkinson, D. (2004) Conformation and lipid binding of the N-terminal (1−44) domain of human apolipoprotein A-I, *Biochemistry 43*, 13156−13164.
33. Fang, Y., Gursky, O., and Atkinson, D. (2003) Structural studies of N- and C-terminally truncated human apolipoprotein A-I, *Biochemistry 42*, 6881−6890.
34. Segrest, J. P., Garber, D. W., Brouillette, C. G., Harvey, S. C., and Anantharamaiah, G. M. (1994) The amphipathic α helix: A multifunctional structural motif in plasma apolipoproteins, *Adv. Protein Chem. 45*, 303−369.
35. Derksen, A., Gantz, D., and Small, D. M. (1996) Calorimetry of apolipoprotein-A1 binding to phosphatidylcholine-triolein-cholesterol emulsions, *Biophys. J. 70*, 330−338.
36. Hevonoja, T., Pentikainen, M. O., Hyvonen, M. T., Kovanen, P. T., and Ala-Korpela, M. (2000) Structure of low-density lipoprotein (LDL) particles: Basis for understanding molecular changes in modified LDL, *Biochim. Biophys. Acta 1488*, 189−210.
37. Epand, R. M., Epand, R. F., Sayer, B. G., Melacini, G., Palgulachari, M. N., Segrest, J. P., and Anantharamaiah, G. M. (2004) An apolipoprotein AI mimetic peptide: Membrane interactions and the role of cholesterol, *Biochemistry 43*, 5073−5083.
38. Wieprecht, T., Apostolov, O., Beyermann, M., and Seelig, J. (1999) Thermodynamics of the α-helix-coil transition of amphipathic peptides in a membrane environment: Implications for the peptide-membrane binding equilibrium, *J. Mol. Biol. 294*, 785−794.
39. Seelig, J. (2004) Thermodynamics of lipid-peptide interactions, *Biochim. Biophys. Acta 1666*, 40−50.
40. Arnulphi, C., Jin, L., Tricerri, M. A., and Jonas, A. (2004) Enthalpy-driven apolipoprotein A-I and lipid bilayer interaction indicating protein penetration upon lipid binding, *Biochemistry 43*, 12258−12264.
41. Gazzara, J. A., Phillips, M. C., Lund-Katz, S., Palgunachari, M. N., Segrest, J. P., Anantharamaiah, G. M., Rodrigueza, W. V., and Snow, J. W. (1997) Effect of vesicle size on their interaction with class A amphipathic helical peptides, *J. Lipid Res. 38*, 2147−2154.
42. Wimley, W. C., and White, S. H. (1993) Membrane partitioning: Distinguishing bilayer effects from the hydrophobic effect, *Biochemistry 32*, 6307−6312.

BI050853+